



Short communication

Selective allylic oxidation of cyclohexene catalyzed by nanostructured Ce-Sm-Si materials



Bolla Govinda Rao^{a,b}, Putla Sudarsanam^c, P.R.G. Nallappareddy^{a,b}, M. Yugandhar Reddy^a,
T. Venkateshwar Rao^{a,b}, Benjaram M. Reddy^{a,b,*}

^a Inorganic and Physical Chemistry Division, CSIR – Indian Institute of Chemical Technology, Uppal Road, Hyderabad 500 007, India

^b Academy of Scientific and Innovative Research, CSIR-IIT, India

^c Leibniz-Institut für Katalyse, Universität Rostock, Albert-Einstein Straße 29A, 18059 Rostock, Germany

ARTICLE INFO

Keywords:

Cyclohexene
Allylic oxidation
Ceria
Samarium
Silica
Redox-acid sites

ABSTRACT

The oxidation of cyclohexene was studied using nanostructured CeO₂, CeO₂/SiO₂, CeO₂-Sm₂O₃, and CeO₂-Sm₂O₃/SiO₂ catalysts. The CeO₂-Sm₂O₃/SiO₂ catalyst shows ~96% cyclohexene conversion and ~91% selectivity to allylic products, namely, 2-cyclohexen-1-one (~53%) and 2-cyclohexen-1-ol (~38%) owing to favorable redox (oxygen vacancies) and acid sites stimulated by synergistic interactions of dopant (Sm) and support (SiO₂) with CeO₂. In contrast, only ~40, ~55, and ~78% of cyclohexene conversions were observed, respectively, over CeO₂, CeO₂/SiO₂, and CeO₂-Sm₂O₃ catalysts. With the increase of reaction time, temperature, and molar ratio of cyclohexene/oxidant, the conversion of cyclohexene and the selectivity of 2-cyclohexen-1-one are increased considerably.

1. Introduction

The oxidation of olefins is an important chemical transformation as the resulting products are key building blocks for the synthesis of fine and bulk chemicals [1–3]. Particularly, the oxidation of cyclohexene yields valuable oxygenated products, such as cyclohexene oxide, 2-cyclohexen-1-ol, and 2-cyclohexen-1-one. Cyclohexene oxide formed through the epoxidation of cyclohexene is a key chemical in the synthesis of polymers, pharmaceuticals, fine chemicals, and biological materials. As well, the allylic oxidation products, namely, 2-cyclohexen-1-ol and 2-cyclohexen-1-one are important intermediates in the manufacture of spices, medication, pesticides, and insect pheromones [4,5]. Traditionally, the oxidation of cyclohexene is performed with the aid of inorganic/organic oxidants, such as iodine benzene, sodium hypochlorite, and chromium trioxide. However, the applicability of these oxidants was strongly restricted due to various concerns, such as higher cost, explosivity, high toxicity, and lower atom economy [6,7]. Moreover, most of the procedures reported for the oxidation of cyclohexene involve the use of metal complexes based on Co, Fe, Mn, Ru and Cu, as well as gold nanoparticles immobilized on different supports [5,6,8–10]. These procedures require tedious workup procedure in the case of metal complexes, while Au catalysts are highly expensive. The development of an efficient green approach that utilizes an inexpensive catalyst along with a mild oxidant is therefore highly

desirable to address the above short comings from the viewpoint of sustainable chemical industry.

Ceria (CeO₂) has been recognized as a promising catalytic material in various oxidation reactions, such as soot oxidation, CO oxidation, and benzylamine oxidation [11–14]. This significance is due to its interesting physicochemical properties, excellent redox ability (Ce⁴⁺ ↔ Ce³⁺), and oxygen vacancy defect sites. Doping of aliovalent metal ions into the CeO₂ lattice and the use of support to disperse ceria particles on it are found to be feasible ways to modify the unique properties of CeO₂, hence improving its catalytic performance. Particularly, the doping of a trivalent metal ion like Sm³⁺ favours the formation of large amounts of oxygen vacancies, due to the charge compensation in the ceria lattice [14]. On the other hand, the dispersion of ceria on a high surface area support, for example, SiO₂ can lead to smaller sized particles, improved specific surface area, and abundant catalytically active sites at the metal/oxide interfaces.

In this work, we have investigated the influence of both dopant (Sm) and support (SiO₂) in modifying the redox and acid properties of CeO₂ for cyclohexene oxidation. For this, we have prepared pure CeO₂, Sm-doped CeO₂ (CeO₂-Sm₂O₃), SiO₂ supported CeO₂ (CeO₂/SiO₂), and Sm-doped CeO₂ dispersed on SiO₂ support (CeO₂-Sm₂O₃/SiO₂) by practicable precipitation methods. The catalytic experiments were performed employing tertiary butyl hydroperoxide (TBHP) and acetonitrile as oxidant and solvent, respectively. The influence of reaction

* Corresponding author at: Inorganic and Physical Chemistry Division, CSIR – Indian Institute of Chemical Technology, Uppal Road, Hyderabad 500 007, India.
E-mail address: bmreddy@iict.res.in (B.M. Reddy).

temperature, molar ratio of cyclohexene/TBHP, and reaction time was also studied in cyclohexene oxidation. Various characterization techniques, namely, XRD, TEM, Raman, XPS, NH_3 -TPD, and BET surface area have been used to investigate the structural, redox, and acid properties of the catalysts.

2. Experimental

The detailed procedure of catalyst synthesis, characterization, and activity are presented in the supporting information.

3. Results and discussion

3.1. Catalyst screening for cyclohexene oxidation

The oxidation of olefins has been demonstrated, choosing cyclohexene as a model compound to assess the catalytic performance of ceria-based materials. The oxidation of cyclohexene typically gives cyclohexene oxide (Cy-Oxide), 2-cyclohexen-1-one (Cy-One), 2-cyclohexen-1-ol (Cy-Ol), and 3-(tert-butylperoxy)cyclohex-1-ene (Cy-TBHP) (Scheme S1). The obtained results in the oxidation of cyclohexene over CeO_2 , $\text{CeO}_2\text{-SiO}_2$, $\text{CeO}_2\text{-Sm}_2\text{O}_3$, and $\text{CeO}_2\text{-Sm}_2\text{O}_3/\text{SiO}_2$ catalysts are shown in Fig. 1. In the case of blank run, the conversion of cyclohexene was found to be very low ($\sim 5\%$), indicating the necessity of the catalyst in cyclohexene oxidation. When the reaction is conducted using pure CeO_2 , the conversion of cyclohexene was increased from ~ 5 to $\sim 40\%$ and a high selectivity to allylic products, namely, Cy-Ol ($\sim 45\%$) and Cy-One ($\sim 40\%$) was observed, with low selectivity of Cy-Oxide ($\sim 8.5\%$) and Cy-TBHP ($\sim 6.5\%$). Cy-Oxide is formed through the epoxidation of cyclohexene, while Cy-TBHP product is an intermediate in both epoxidation and allylic oxidation of cyclohexene as shown in Scheme 1. The $\text{CeO}_2/\text{SiO}_2$ catalyst shows a considerable improvement in the cyclohexene conversion ($\sim 55\%$) compared to pure CeO_2 ($\sim 40\%$), however, there was no variation in the selectivity of Cy-Ol ($\sim 44\%$) and Cy-One ($\sim 42\%$). When the reaction was conducted using $\text{CeO}_2\text{-Sm}_2\text{O}_3$, the conversion of cyclohexene was considerably increased from ~ 40 (obtained over pure CeO_2) to $\sim 78\%$, indicating the key role of Sm dopant in improving the catalytic performance of CeO_2 in cyclohexene oxidation. The conversion of cyclohexene was tremendously improved with the addition of dopant (Sm) and support (SiO_2) to pure CeO_2 : $\sim 96\%$ cyclohexene conversion was found over $\text{CeO}_2\text{-Sm}_2\text{O}_3/\text{SiO}_2$ catalyst. This result clearly indicates co-operative effect of Sm and SiO_2 in improving the efficiency of ceria for this reaction. A high selectivity to allylic oxidation products, namely Cy-One ($\sim 53\%$) and Cy-Ol ($\sim 38\%$) were found over $\text{CeO}_2\text{-Sm}_2\text{O}_3/\text{SiO}_2$ catalyst. It was therefore clear from Fig. 1 that all the catalysts show a high selectivity towards allylic oxidation of cyclohexene. To specifically understand the efficiency of the catalysts, the turnover frequency (TOF) values were calculated using the expression “moles of cyclohexene converted per

mol of catalyst per hour”. It was found that the $\text{CeO}_2\text{-Sm}_2\text{O}_3/\text{SiO}_2$ catalyst shows a high TOF value (5.6×10^{-3}) followed by $\text{CeO}_2\text{-Sm}_2\text{O}_3$ (4.1×10^{-3}), $\text{CeO}_2\text{-SiO}_2$ (1.28×10^{-3}), and CeO_2 (0.69×10^{-3}). The obtained TOF values clearly indicate the better performance of $\text{CeO}_2\text{-Sm}_2\text{O}_3/\text{SiO}_2$ catalyst in cyclohexene oxidation. Since $\text{CeO}_2\text{-Sm}_2\text{O}_3/\text{SiO}_2$ catalyst shows a high performance in cyclohexene oxidation, we studied the effect of temperature, mole ratio of cyclohexene/TBHP, and reaction time in cyclohexene oxidation.

3.2. Influence of reaction temperature

The oxidation of cyclohexene was carried out in the range of 313–353 K over $\text{CeO}_2\text{-Sm}_2\text{O}_3/\text{SiO}_2$ catalyst (Fig. S1). The conversion of cyclohexene was found to be very low ($\sim 28\%$) at 313 K and a high selectivity of Cy-Ol ($\sim 48\%$) was observed compared to Cy-One ($\sim 34\%$). As the temperature increases from 313 to 353 K, the conversion of cyclohexene is significantly increased from ~ 28 to 96% , respectively. Interestingly, when the temperature is increased from 313 to 353 K the selectivity of Cy-Ol is decreased from 48 to 38% with the increase of Cy-One selectivity from ~ 34 to $\sim 53\%$, respectively. In addition, the selectivity of epoxidation product i.e. Cy-Oxide is decreased from ~ 10.7 to $\sim 5\%$ with the increase of temperature from 313 to 353 K. This observation suggests that the reaction temperature plays a huge effect in the conversion of cyclohexene and the products selectivity.

3.3. Influence of reaction time

We have undertaken the reaction at different time intervals at 353 K over $\text{CeO}_2\text{-Sm}_2\text{O}_3/\text{SiO}_2$ catalyst (Table 1). The achieved cyclohexene conversions are ~ 30 , ~ 58 , ~ 79 , and $\sim 96\%$ for 1, 2, 3, and 4 h of reaction times, respectively. For 1 h, a high selectivity to Cy-Ol ($\sim 50\%$) was found followed by Cy-One ($\sim 28\%$), Cy-Oxide ($\sim 12\%$), and Cy-TBHP ($\sim 10\%$). When the reaction time is increased to 4 h, the relative selectivity ratio of Cy-Ol and Cy-One was found to decrease i.e., a $\sim 53\%$ of Cy-One selectivity was found, while only $\sim 38\%$ of Cy-Ol is noted. In addition, a small decrease in the selectivity of Cy-Oxide and Cy-TBHP products was found with the increase of reaction time (Table 1).

3.4. Influence of cyclohexene/TBHP molar ratio

The effect of cyclohexene/TBHP molar ratio was investigated in cyclohexene oxidation over $\text{CeO}_2\text{-Sm}_2\text{O}_3/\text{SiO}_2$ catalyst at 353 K (Fig. 2). The cyclohexene conversion was found to be poor ($\sim 28\%$) at low cyclohexene/TBHP mole ratio (1:0.25), which is due to less availability of TBHP molecules to interact with cyclohexene molecules. With the increase of cyclohexene/TBHP molar ratio, the conversion of cyclohexene was increased: the achieved cyclohexene conversions are ~ 28 , ~ 54 ,

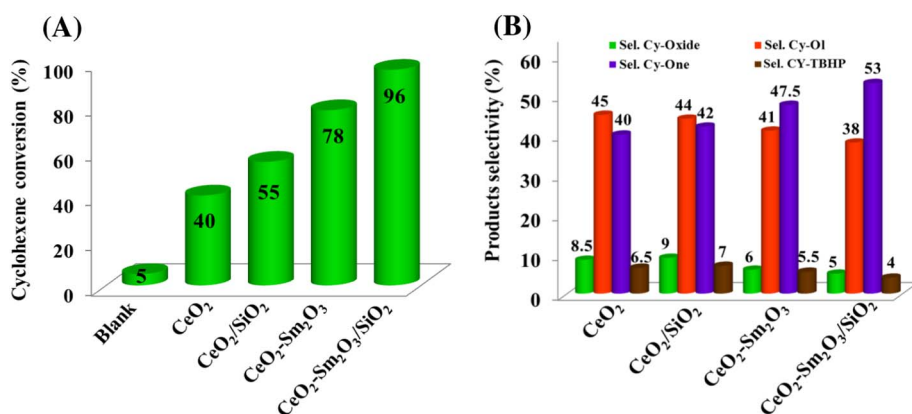
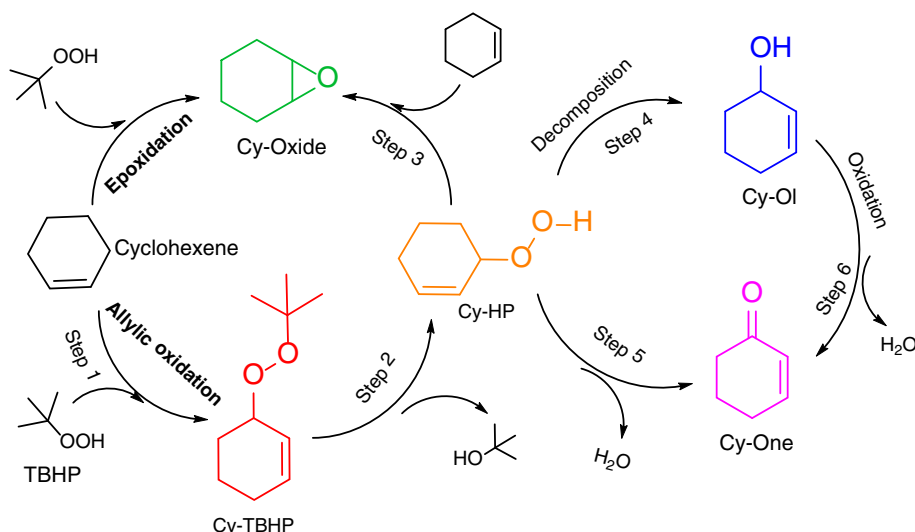


Fig. 1. Selective oxidation of cyclohexene over CeO_2 , $\text{CeO}_2/\text{SiO}_2$, $\text{CeO}_2\text{-Sm}_2\text{O}_3$, and $\text{CeO}_2\text{-Sm}_2\text{O}_3/\text{SiO}_2$ catalysts: (A) conversion of cyclohexene and (B) selectivity of cyclohexene oxide (Cy-Oxide), 2-cyclohexen-1-ol (Cy-Ol), 2-cyclohexen-1-one (Cy-One), and 3-(tert-butylperoxy)cyclohex-1-ene (Cy-TBHP).



Scheme 1. Plausible reaction pathways for the cyclohexene oxidation.

Table 1

Influence of reaction time on the cyclohexene oxidation over $\text{CeO}_2\text{-Sm}_2\text{O}_3/\text{SiO}_2$ catalyst: conversion of cyclohexene and selectivity of cyclohexene oxide (Cy-Oxide), 2-cyclohexen-1-ol (Cy-Ol), 2-cyclohexen-1-one (Cy-One), and 3-(tert-butylperoxy)cyclohex-1-ene (Cy-TBHP).

Time (h)	Cyclohexene conversion (%)	Sel. of Cy-TBHP (%)	Sel. of Cy-Oxide (%)	Sel. of Cy-Ol (%)	Sel. of Cy-One (%)
1	30	10	12	50	28
2	58	6	8	46	40
3	79	5	6	41	48
4	96	4	5	38	53

~82, and ~96% for 1:0.25, 1:0.50, 1:0.75, and 1:1 mol ratios, respectively. At 1:0.25 molar ratio of cyclohexene/TBHP, considerable amount of epoxidation product, Cy-Oxide (~26%) was obtained, which is found to decrease to 5% with the increase of molar ratio of cyclohexene/TBHP to 1:1. In parallel, the selectivity of Cy-One is increased from ~24, ~40, ~41.5 to ~55% with the increase of cyclohexene/TBHP molar ratio from 1:0.25, 1:0.50, 1:0.75 to 1:1, respectively. It was obvious from Figs. 1, 2, S1, and Table 1 that the selectivity of the products is highly dependent on the molar ratio of cyclohexene/TBHP compared to temperature and time.

4. Physicochemical characterization

The high catalytic performance of $\text{CeO}_2\text{-Sm}_2\text{O}_3/\text{SiO}_2$ material could be attributed to several factors, for example, high specific surface area,

abundant redox sites, and strong acid sites. To understand this, we have characterized the materials using various analytical techniques and the results are shown in the following paragraphs.

Fig. S2 shows Raman spectra of the samples. A sharp band was found at $\sim 465\text{ cm}^{-1}$ for all the samples, which is due to F_{2g} Raman active mode of fluorite structured CeO_2 [15]. No Raman bands were observed for dopant oxide (Sm_2O_3) and SiO_2 support. A shifting of F_{2g} peak towards lower wavenumbers was found for $\text{CeO}_2\text{-Sm}_2\text{O}_3$, $\text{CeO}_2\text{-SiO}_2$, and $\text{CeO}_2\text{-Sm}_2\text{O}_3/\text{SiO}_2$ samples compared to CeO_2 . The peak shifting is more predominant in the case of $\text{CeO}_2\text{-Sm}_2\text{O}_3/\text{SiO}_2$ sample. The doping of heterovalent metal ion like Sm^{3+} leads to perturbations in the CeO_2 lattice due to difference in the ionic radii of Ce^{4+} (0.97 Å) and Sm^{3+} (1.08 Å), thus variations in the frequency of Ce–O bond and F_{2g} band shifting in doped CeO_2 materials compared to that of bare CeO_2 are apparent [11,16–18]. Two more Raman bands were noticed for $\text{CeO}_2\text{-Sm}_2\text{O}_3$ and $\text{CeO}_2\text{-Sm}_2\text{O}_3/\text{SiO}_2$ samples. The appearance of a band at $\sim 560\text{ cm}^{-1}$ indicates the presence of oxygen vacancies, whereas the band at $\sim 606\text{ cm}^{-1}$ reveals SmO_8 defect complex [19–21]. The estimated concentration of oxygen vacancies (O_v/F_{2g} , Table S1) indicates that the $\text{CeO}_2\text{-Sm}_2\text{O}_3/\text{SiO}_2$ catalyst has more number of oxygen vacancies ($\text{O}_v/\text{F}_{2g} = 0.1053$) compared to $\text{CeO}_2\text{-Sm}_2\text{O}_3$ catalyst ($\text{O}_v/\text{F}_{2g} = 0.0948$).

Fig. S3 shows XRD patterns of prepared samples. All the samples exhibit characteristic reflections of fluorite cubic structured CeO_2 [22]. No XRD peaks pertaining to Sm_2O_3 are found, which is due to several factors, such as incorporation of Sm^{3+} ions into the ceria lattice, amorphous nature of Sm_2O_3 , and high dispersion of Sm_2O_3 species in the synthesized catalysts [14,23–25]. As well, no peaks corresponding to SiO_2 were observed, revealing amorphous nature of SiO_2 . The

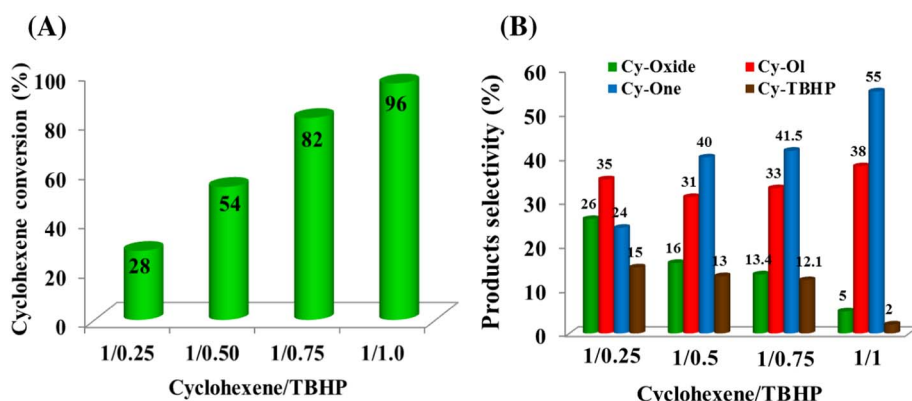


Fig. 2. Influence of cyclohexene/TBHP mole ratio on cyclohexene oxidation over $\text{CeO}_2\text{-Sm}_2\text{O}_3/\text{SiO}_2$ catalyst: (A) conversion of cyclohexene and (B) selectivity of cyclohexene oxide (Cy-Oxide), 2-cyclohexen-1-ol (Cy-Ol), 2-cyclohexen-1-one (Cy-One), and 3-(tert-butylperoxy)cyclohex-1-ene (Cy-TBHP).

estimated average crystallite sizes of the samples reveal that the $\text{CeO}_2\text{-Sm}_2\text{O}_3/\text{SiO}_2$ sample has smaller crystallites (~ 5.1 nm), due to high dispersion of $\text{CeO}_2\text{-Sm}_2\text{O}_3$ crystallites on the SiO_2 surface (Table S1). The N_2 -adsorption/desorption isotherms of the samples are shown in Fig. S4. All samples show type IV isotherm with H1 hysteresis loop, revealing mesoporous nature of the materials [25]. The BET surface area of the samples is presented in Table S1. The $\text{CeO}_2\text{-Sm}_2\text{O}_3/\text{SiO}_2$ catalyst exhibits large BET surface area ($193\text{ m}^2/\text{g}$) followed by $\text{CeO}_2/\text{SiO}_2$ ($120\text{ m}^2/\text{g}$), $\text{CeO}_2\text{-Sm}_2\text{O}_3$ ($78\text{ m}^2/\text{g}$), and CeO_2 ($39\text{ m}^2/\text{g}$). These results indicate favorable role of dopant (Sm) and support (SiO_2) in enhancing the surface area of CeO_2 .

Fig. S5 shows TEM images of prepared samples. All samples exhibit nearly spherical shaped particles and fall in the nanoscale range ($\sim 8\text{--}12$ nm). The estimated d-spacings for the lattice fringes of the materials were found to be ~ 0.31 nm, corresponding to the distance between the adjacent (111) crystal planes of fluorite-structured CeO_2 [26]. Fig. S6 displays Ce 3d XP spectra of ceria samples. The peaks assigned with u indicate $3d_{3/2}$ spin-orbit states and those labeled by 'v' correspond to $3d_{5/2}$ contributions. As shown in Fig. S6, the peaks labeled by u' and v' represent the Ce^{3+} , whereas bands labeled with u, u'', u''', v, v'', and v''' correspond to Ce^{4+} . The presence of all these peaks reveal the coexistence of Ce^{4+} and Ce^{3+} ions over the surface of the samples [27].

The Sm $3d_{5/2}$ XP spectra of the $\text{CeO}_2\text{-Sm}_2\text{O}_3$ and $\text{CeO}_2\text{-Sm}_2\text{O}_3/\text{SiO}_2$ samples show two peaks (Fig. S7). The peak at higher binding energy indicates the Sm^{3+} oxidation state, while the peak at lower binding energy corresponds to the charge transfer effect of the unpaired 4f electrons in Sm-oxide [14]. Fig. S8 shows O 1s XP spectra of the samples. The appearance of peak at lower binding energy ($525\text{--}530\text{ cm}^{-1}$) denotes the ceria lattice oxygen [25]. In contrast, the higher binding energy peak ($532\text{--}534\text{ cm}^{-1}$) is attributed to adsorbed oxygen species on the catalyst surface. Si 2p core level XP spectra of $\text{CeO}_2/\text{SiO}_2$ and $\text{CeO}_2\text{-MoO}_3/\text{SiO}_2$ catalysts show a peak at ~ 102.8 eV, which is attributed to SiO_2 (Fig. S9) [28]. The NH_3 -TPD results of the samples are shown in Fig. 3. All the samples exhibit three peak maxima, due to the differences in the desorption activation energy of NH_3 from different types of acidic sites present in the catalyst [29–31]. The higher the temperature of desorption, the more acidic the acid site is. It was

obvious from Fig. 3 that the $\text{Ce-Sm}/\text{SiO}_2$ sample shows two peak maxima at higher temperatures (646 and 744 K), while only one peak maxima was found for Ce-Sm (653 K) and Ce/SiO_2 (705 K) samples. This indicates that the $\text{Ce-Sm}/\text{SiO}_2$ sample shows large amounts of strong acidic sites, which could play a key role in cyclohexene oxidation as discussed in the later paragraphs.

5. Reaction pathways and structure-activity properties in cyclohexene oxidation

Based on our experimental results and literature reports, plausible reaction pathways for the cyclohexene oxidation were proposed (Scheme 1) [4,32–34]. The oxidation of cyclohexene with TBHP produces cyclohexene oxide (Cy-Oxide) through epoxidation process. At the same time, cyclohexene could react with TBHP, facilitating 3-(tert-butylperoxy)cyclohex-1-ene (Cy-TBHP, step 1), which readily undergoes decomposition to yield 2-cyclohexen-1-hydroperoxide (Cy-HP) with the elimination of tertiary butyl alcohol (step 2). 2-Cyclohexene-1-hydroperoxide can also yield cyclohexene oxide (Cy-Oxide) through the epoxidation of cyclohexene (step 3). Meanwhile, 2-cyclohexen-1-hydroperoxide (CY-HP) can decompose upon heating to yield 2-cyclohexen-1-ol (Cy-OL, step 4) as well as to cyclohexen-1-one (Cy-One, step 5) by the elimination of water, which is acid catalyzed reaction [35,36]. Cyclohexen-1-one (Cy-One) and H_2O (byproduct) can be also formed via the oxidation of 2-cyclohexen-1-ol (Cy-OL, step 6).

Activity results reveal that a high selectivity of allylic products, namely, 2-cyclohexen-1-one and 2-cyclohexen-1-ol were formed in the oxidation of cyclohexene (Fig. 1B). This indicates that ceria catalysts show a high selectivity towards allylic products compared to epoxidation products. As shown in Scheme 1, 2-cyclohexen-1-one is formed by dehydration of 2-cyclohexen-1-hydroperoxide (Cy-HP, step 5) as well as by oxidation of 2-cyclohexen-1-ol (Cy-OL, step 6), which are typically catalyzed by acid and redox sites, respectively. Among the catalysts tested, the $\text{CeO}_2\text{-Sm}_2\text{O}_3/\text{SiO}_2$ catalyst shows a high selectivity towards 2-cyclohexen-1-one ($\sim 53\%$) compared to 2-cyclohexen-1-ol ($\sim 38\%$). Raman (Fig. S2) and NH_3 -TPD (Fig. 3) studies reveal that the $\text{CeO}_2\text{-Sm}_2\text{O}_3/\text{SiO}_2$ catalyst shows improved structural properties and strong acid sites, respectively, hence high catalytic performance of $\text{CeO}_2\text{-Sm}_2\text{O}_3/\text{SiO}_2$ in cyclohexene oxidation with high selectivity of 2-cyclohexen-1-one. In addition, the high BET surface area of the $\text{CeO}_2\text{-Sm}_2\text{O}_3/\text{SiO}_2$ catalyst ($193\text{ m}^2/\text{g}$) is also a key factor in achieving better results in cyclohexene oxidation reaction. Further studies are under investigation to optimize the structural, redox and acid properties of ceria-based catalysts to achieve better results in cyclohexene oxidation.

6. Conclusions

In summary, nanoscale CeO_2 , $\text{CeO}_2/\text{SiO}_2$, $\text{CeO}_2\text{-Sm}_2\text{O}_3$, and $\text{CeO}_2\text{-Sm}_2\text{O}_3/\text{SiO}_2$ materials were developed for selective allylic oxidation of cyclohexene. The achieved cyclohexene conversions over various catalysts were: $\text{CeO}_2\text{-Sm}_2\text{O}_3/\text{SiO}_2$ ($\sim 96\%$) > $\text{CeO}_2\text{-Sm}_2\text{O}_3$ ($\sim 78\%$) > $\text{CeO}_2/\text{SiO}_2$ ($\sim 55\%$) > CeO_2 ($\sim 40\%$). Irrespective of the catalyst tested, a high selectivity towards allylic products, namely, 2-cyclohexen-1-one and 2-cyclohexen-1-ol were found compared to epoxidation product (cyclohexene oxide). Characterization studies reveal that the presence of high BET surface area, improved structural properties and abundant acid sites stimulated by synergistic interactions of Sm and SiO_2 with CeO_2 are the key factors for high efficiency of $\text{CeO}_2\text{-Sm}_2\text{O}_3/\text{SiO}_2$ catalyst in cyclohexene oxidation.

Acknowledgments

BG and PNG thank the Council of Scientific and Industrial Research (CSIR), New Delhi for research fellowships. Financial support for this project was received from Department of Science and Technology, New Delhi, under SERB Scheme (SB/S1/PC-106/2012).

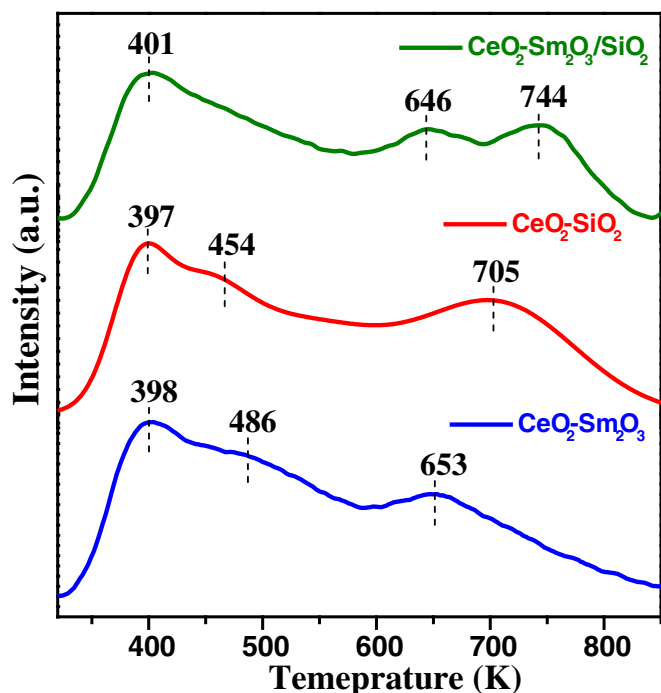


Fig. 3. NH_3 -TPD profiles of $\text{CeO}_2/\text{SiO}_2$, $\text{CeO}_2\text{-Sm}_2\text{O}_3$ and $\text{CeO}_2\text{-Sm}_2\text{O}_3/\text{SiO}_2$ catalysts.

Appendix A. Supplementary data

Catalysts characterization, catalysts synthesis, and characterization results of the samples, activity results and scheme for the cyclohexene oxidation are presented in the Supporting information. Supplementary data associated with this article can be found in the online version, at <http://dx.doi.org/10.1016/j.catcom.2017.07.027>.

References

- [1] Y. Cao, H. Yu, H. Wang, F. Feng, *Catal. Commun.* 88 (2017) 99–103.
- [2] F. Parra da Silva, R.V. Gonçalves, L.M. Rossi, *J. Mol. Catal. A Chem.* 426 (2017) 534–541.
- [3] Y. Cao, H. Yu, F. Peng, H. Wang, *ACS Catal.* 4 (2014) 1617–1625.
- [4] J. Tong, W. Wang, L. Su, Q. Li, F. Liu, W. Ma, Z. Lei, L. Bo, *Catal. Sci. Technol.* 7 (2017) 222–230.
- [5] Q.X. Luo, M. Ji, S.E. Park, C. Hao, Y.Q. Li, *RSC Adv.* 6 (2016) 33048–33054.
- [6] D. Yang, T. Jiang, T. Wu, P. Zhang, H. Han, B. Han, *Catal. Sci. Technol.* 6 (2016) 193–200.
- [7] I.Y. Skobelev, A.B. Sorokin, K.A. Kovalenko, V.P. Fedin, *J. Catal.* 298 (2013) 61–69.
- [8] A. Abdolmaleki, S.R. Adariani, *Catal. Commun.* 59 (2015) 97–100.
- [9] M. Bagherzadeh, A. Ghanbarpour, H.R. Khavasi, *Catal. Commun.* 65 (2015) 72–75.
- [10] B.G. Donoeva, D.S. Ovoshchnikov, V.B. Golovko, *ACS Catal.* 3 (2013) 2986–2991.
- [11] P. Sudarsanam, B. Hillary, B. Mallesham, B. Govinda Rao, M.H. Amin, A. Nafady, A.M. Alsalmeh, B.M. Reddy, S.K. Bhargava, *Langmuir* 32 (2016) 2208–2215.
- [12] W.W. Wang, W.Z. Yu, P.P. Du, H. Xu, Z. Jin, R. Si, C. Ma, S. Shi, C.J. Jia, C.H. Yan, *ACS Catal.* 7 (2017) 1313–1329.
- [13] B. Govinda Rao, P. Sudarsanam, B. Mallesham, B.M. Reddy, *RSC Adv.* 6 (2016) 95252–95262.
- [14] P. Sudarsanam, A. Rangaswamy, B.M. Reddy, *RSC Adv.* 4 (2014) 46378–46382.
- [15] P. Sudarsanam, B. Hillary, M.H. Amin, S.B.A. Hamid, S.K. Bhargava, *Appl. Catal. B Environ.* 185 (2016) 213–224.
- [16] D.W. Wheeler, I. Khan, *Vib. Spectrosc.* 70 (2014) 200–206.
- [17] D. Mukherjee, B. Govinda Rao, B.M. Reddy, *Appl. Catal. B Environ.* 197 (2016) 105–115.
- [18] B. Hillary, P. Sudarsanam, M.H. Amin, S.K. Bhargava, *Langmuir* 33 (2017) 1743–1750.
- [19] L. Li, F. Chen, J.-Q. Lu, M.-F. Luo, *J. Phys. Chem. A* 115 (2011) 7972–7977.
- [20] K. Kuntaiah, P. Sudarsanam, B.M. Reddy, A. Vinu, *RSC Adv.* 3 (2013) 7953–7962.
- [21] T. Taniguchi, T. Watanabe, N. Sugiyama, A.K. Subramani, H. Wagata, N. Matsushita, M. Yoshimura, *J. Phys. Chem. C* 113 (2009) 19789–19793.
- [22] T.H. Vuong, J. Radnik, J. Rabeah, U. Bentrup, M. Schneider, H. Atia, U. Armbruster, W. Grünert, A. Brückner, *ACS Catal.* 7 (2017) 1693–1705.
- [23] A.G.M. Silva, T.S. Rodrigues, A. Dias, H.V. Fajardo, R.F. Gonçalves, M. Godinho, P.A. Robles-Dutenhefner, *Catal. Sci. Technol.* 4 (2014) 814–821.
- [24] M. Guo, J. Lu, Y. Wu, Y. Wang, M. Luo, *Langmuir* 27 (2011) 3872–3877.
- [25] P. Sudarsanam, K. Kuntaiah, B.M. Reddy, *New J. Chem.* 38 (2014) 5991–6001.
- [26] Y. Zhang, C. Chen, W. Gong, J. Song, H. Zhang, Y. Zhang, G. Wang, H. Zhao, *Catal. Commun.* 93 (2017) 10–14.
- [27] B. Govinda Rao, D. Jampaiah, P. Venkataswamy, B.M. Reddy, *ChemistrySelect* 1 (2016) 6681–6691.
- [28] S. Zhu, X. Gao, Y. Zhu, W. Fan, J. Wang, Y. Li, *Catal. Sci. Technol.* 5 (2015) 1169–1180.
- [29] M.L. Testa, V.L. Parola, L.F. Liotta, A.M. Venezia, *J. Mol. Catal. A Chem.* 367 (2013) 69–76.
- [30] R. Zhang, Q. Zhong, W. Zhao, *Res. Chem. Intermed.* 41 (2015) 3479.
- [31] B. Govinda Rao, P. Sudarsanam, A. Rangaswamy, B.M. Reddy, *Catal. Lett.* 145 (2015) 1436–1445.
- [32] P. Bujak, P. Bartczak, J. Polanski, *J. Catal.* 295 (2012) 15–21.
- [33] X. Cai, H. Wang, Q. Zhanga, J. Tonga, Z. Lei, *J. Mol. Catal. A Chem.* 383–384 (2014) 217–224.
- [34] Y. Chang, Y. Lv, F. Lu, F. Zha, Z. Lei, *J. Mol. Catal. A Chem.* 320 (2010) 56–61.
- [35] Y.N. Wei, H. Li, F. Yue, Q. Xu, J.D. Wang, Y. Zhang, *RSC Adv.* 6 (2016) 107104–107108.
- [36] S. El-Korso, S. Bedrane, A. Choukchou-Braham, R. Bachir, *RSC Adv.* 5 (2015) 63382–63392.